Physiological and Molecular Plant Pathology 142 (2026) 103072

Contents lists available at ScienceDirect

Physiological and Molecular Plant Pathology

journal homepage: www.elsevier.com/locate/pmpp

Identification of the biosynthetic gene cluster for desmethylmensacarcin, a phytotoxic polyketide produced by *Streptomyces niveiscabiei* ST1015

María Inés Lapaz [a], Sofia Zeballos-Gorón [a], Valentina Croce [a], José Carlos Huguet-Tapía [b], Martín Pérez-Baldassari [a], Andrés López [c], Donald Hudson [d], Sarah Forester [e], Rosemary Loria [b], Guillermo Moyna [c], María Julia Pianzzola [a], María Inés Siri [a,*], Isolde M. Francis [d,**]

[a] Área Microbiología, Departamento de Biociencias, Facultad de Química, Universidad de La República, Montevideo, CP 11800, Uruguay
[b] Department of Plant Pathology, Institute of Food and Agricultural Sciences, University of Florida, Gainesville, FL, 32611, USA
[c] Laboratorio de Química Orgánica, Departamento de Química Del Litoral, CENUR Litoral Norte, Universidad de La República, Paysandú, 60000, Uruguay
[d] Department of Biology, California State University, Bakersfield, CA, 93311, USA
[e] Department of Chemistry and Biochemistry, California State University, Bakersfield, CA, 93311, USA

ARTICLE INFO

Keywords:
Biosynthetic gene cluster
Common scab
Genome mining
Virulence

ABSTRACT

This work reports the first functional characterization of the biosynthetic gene cluster (BGC) responsible for the production of the phytotoxic polyketide desmethylmensacarcin (dmsn) in *Streptomyces niveiscabiei* ST1015, a potato common scab pathogen. Using genome sequencing and comparative analysis, a 22-gene type II polyketide synthase (PKS) cluster was discovered with high identity to the mensacarcin (msn) cluster from *Streptomyces bottropensis* but lacking the three methyltransferase genes (msnM1–M3), confirming dmsn as the final product. Dmsn production was detected only in plant-based media and correlated with phytotoxic activity in radish seedling and potato tuber assays. Quantitative analysis based on seedling length ratios relative to the water control showed a ~90 % reduction in the phytotoxic effect of culture supernatants from the mutants lacking the core ketosynthase genes (*dmsnK1–K2*) compared to the wild type ($p < 0.001$). Genetic complementation of the mutants restored the phytotoxicity to wild-type levels. Surprisingly, the mutant strains remained virulent on potato, suggesting that dmsn is not the sole determinant of pathogenicity in ST1015. BiG-SCAPE analysis revealed that msn/dmsn-like BGCs are more widely distributed among pathogenic *Streptomyces species* than previously recognized, although some strains carry non-functional clusters due to premature stop codons or possible regulatory divergence. These findings suggest that multiple potentially redundant phytotoxic pathways may contribute to common scab pathogenesis. This work highlights the widespread occurrence and functional diversity of dmsn-like clusters and provides new insights into the ecological and genetic complexity underlaying common scab pathogenesis.

1. Introduction

Potato common scab (CS) is a widespread disease occurring in practically all potato growing areas around the world. Typical necrotic and corky lesions form on the surface of the tubers, ranging from raised to deep-pitted lesions which significantly reduce the market value of the tubers. A limited understanding of the environmental factors conducive to the disease and the lack of disease-resistant potato cultivars, but also the variability among the disease-causing pathogens contributes to the difficulty of managing the disease [1].

Several potato CS pathogens have been identified and belong to the filamentous bacterial genus *Streptomyces*. This large genus of ubiquitous soil-inhabiting bacteria comprises mostly saprophytic bacteria that are well-known for their ability to degrade large recalcitrant polymers such as cellulose and chitin, and the production of diverse secondary metabolites with a wide range of applications in the health care and agricultural sector [2]. Among the CS pathogens within this genus, *S. scabiei*, *S. acidiscabies*, *S. turgidiscabies*, and *S. ipomoeae* are the best-studied species. For these *Streptomyces* species, pathogenicity is mainly accomplished through the production of one or more thaxtomin phytotoxins

* Corresponding author.
** Corresponding author.
E-mail addresses: msiri@fq.edu.uy (M.I. Siri), ifrancis@csub.edu (I.M. Francis).

https://doi.org/10.1016/j.pmpp.2025.103072
Received 16 July 2025; Received in revised form 28 November 2025; Accepted 1 December 2025
Available online 5 December 2025

[3,4]. Thaxtomins constitute a family of nitrated diketopiperazines derived from L-phenylalanine and 4-nitrotryptophan [5,6]. Thaxtomin A is the most common toxin and acts as an inhibitor of the cellulose synthase complex in actively growing root tissue [5,7]. Besides this well-established pathogenicity determinant, CS pathogens lacking the thaxtomin biosynthetic genes have been reported [8–10]. Moreover, other phytotoxic secondary metabolites involved in potato common scab have been described including one or more coronatine-like compounds, concanamycins, FD-891, borrelidin, and fridamycin E [11–14].

Streptomyces niveiscabiei is another pathogenic species that causes CS in potatoes. It was originally reported in Korea in 2003, leading to its designation as a new *Streptomyces* species [15,16]. Subsequent findings of this species have been reported in Uruguay and China [10,17]. Previous work identified two pathogenic *S. niveiscabiei* strains ST1015 and ST1020, isolated from potato scab lesions in Uruguay during a severe outbreak of CS disease in 2010 displaying particularly deep scab lesions leading to losses of 29 % of the total potato cultivation [10,18,19]. These pathogenic strains lacked the thaxtomin biosynthetic genes as well as *nec1* and *tomA* [10] coding for two virulence factors commonly found together with the thaxtomin biosynthetic cluster and located within the mobile pathogenicity island of pathogenic streptomycetes [20]. The polyketide desmethylmensacarcin (dmsn) was isolated from the supernatant of ST1015, the most aggressive of the two strains and was shown to be more potent than thaxtomin A in causing deep necrotic lesions on potato tuber disks. Culture supernatant also inhibited root and shoot growth of radish seedlings [19]. Dmsn, together with its methylated derivative mensacarcin (msn), was previously isolated from *Streptomyces bottropensis* strain Gö C4/4 [21]. While the biological activity of dmsn remains largely unexplored, the antitumor activity of msn through induction of mitochondrial toxicity and apoptosis is well-documented [21,22].

However, the genetic basis of dmsn biosynthesis and its role in the pathogenicity of *S. niveiscabiei* remain unknown. Moreover, the distribution and functionality of msn/dmsn-like clusters among pathogenic *Streptomyces species* have not been investigated.

This study aimed to identify and functionally characterize the biosynthetic gene cluster (BGC) responsible for the production of the phytotoxic secondary metabolite desmethylmensacarcin (dmsn) in *S. niveiscabiei*. The specific objectives were to (i) determine the genetic organization and confirm the function of the cluster through mutagenesis and complementation, (ii) evaluate the contribution of dmsn to phytotoxicity and virulence, and (iii) explore the occurrence of related clusters among other pathogenic *Streptomyces* species. By addressing these questions, this work contributes to a deeper understanding of the molecular and ecological determinants of virulence in *S. niveiscabiei*.

2. Material and methods

2.1. Bacterial strains and culture conditions

All bacterial strains and plasmids used in this study are listed in Table S1. *Escherichia coli* strains were cultured in Luria-Bertani (LB, Sigma-Aldrich, St. Louis, MO, USA) medium at 37 °C. *Streptomyces* strains were routinely cultured in Tryptic Soy Broth (TSB, BD Biosciences, Franklin Lakes, NJ, USA) or on International *Streptomyces* Project Medium 4 (ISP-4, BD Difco™, BD Biosciences, Franklin Lakes, NJ, USA) at 28 °C. Conjugation was performed on Soy Flour Mannitol (SFM) agar consisting of 20 g/L of each mannitol, soy flour, and agar. After autoclaving, $MgCl_2$ was added to reach a final concentration of 10 mM. Where required, the medium was supplemented with the antibiotic kanamycin (50 μg/mL), apramycin (100 μg/mL), nalidixic acid (50 μg/mL), thiostrepton (50 μg/mL), and/or chloramphenicol (25 μg/mL) (Gold Biotechnology, ST. Louis, MO, USA) [23].

2.2. Genomic DNA extraction

Genomic DNA was extracted as described by Francis et al. [23] but with the addition of a 30-min incubation at 37 °C with 2.5 μL RNase A (Gold Biotechnology, ST. Louis, MO, USA) at a concentration of 10 mg/mL before the genomic DNA was precipitated. The quantity and quality of the DNA preparations were measured using a NanoDrop™ One© Microvolume UV–Vis Spectrophotometer (Thermo Fisher Scientific, Waltham, MA, USA) and agarose gel electrophoresis with 0.5 μg/mL GoodView™ nucleic acid stain (SBS Genetech, China). The extracted DNA was stored at −20 °C until further use.

2.3. Genome sequencing

The genome of *S. niveiscabiei* ST1015 was resequenced using the Oxford Nanopore Technologies (ONT) platform. Sequencing was conducted on a MinION R9.4.1 flow cell [24] using the Rapid Sequencing Kit (SQK-RAD004, Oxford Nanopore Technologies, Oxford, UK) for 10 h using 400 ng of high molecular weight genomic DNA. A total of 1,776,177,308 bases were generated corresponding to a 177x coverage of the genome. The reads had a median of 1132 bp and a median quality score of 8.7 (~85 % accuracy). Assembly was conducted using the Canu v2.0 [25]. Long reads were realigned to the consensus assembly, and a correction was conducted using the Nanopolish v0.14 tool [26]. A second correction was conducted with Illumina reads (Novogene) using the Pilon v1.4 tool [27]. The final consensus assembly was a single contig of 10.17 Mb (RefSeq GCF_003268535.2).

The genomes of *S. niveiscabiei* ST1020 and *S. acidiscabies* ST105 were obtained using a hybrid approach combining long and short reads. Long reads were obtained using a MinION flow cell [24] with the Ligation Sequencing Kit v14 (SQK-LSK114, Oxford Nanopore Technologies, Oxford, UK) for 22 h using 400 ng of high molecular weight genomic DNA. The genomes were assembled using Flye (v2.9.2-b1786) [28] and polished with the long reads using Medaka v1.6.0 (https://github.com/nanoporetech/medaka, accessed July 15, 2024). The obtained genomes were further polished using short reads obtained via Illumina (Novogene, China) with the assistance of Polypolish v0.5.0 [29]. For the genome of ST1020, a total of 460,271,350 bases were generated, equating to a 44x coverage. The final consensus assembly comprised 64 contigs, with a total length of 10.04 Mb (RefSeq GCF_003268555.2). For the genome of ST105, a total of 682,123,055 bases were generated, providing a 62x coverage. The final consensus assembly consisted of 4 contigs, with a total length of 11.07 Mb (RefSeq GCF_003584805.2).

2.4. Search, annotation, and comparison of the dmsn biosynthetic gene cluster (BGC)

The newly generated genomes of *S. niveiscabiei* ST1015 (RefSeq GCF_003268535.2), *S. niveiscabiei* ST1020 (RefSeq GCF_003268555.2), *S. acidiscabies* ST105 (RefSeq GCF_003584805.2), alongside the pathogenic *Streptomyces* genomes downloaded from NCBI (Table S2), were analyzed using the antiSMASH 7.0 software [30]. The BGCs clustering was performed using BiGSCAPE [31]. The identified gene cluster family (GCF) showing the presence of the type II PKS cluster coding for msn production in *S. bottropensis* Gö C4/4 (GenBank accession number KJ437437) was compared using the CAGECAT v1 tool [32]. Gene-to-gene alignments were conducted using Geneious Prime 2023.1.2 (https://www.geneious.com, accessed July 15, 2024).

2.5. Generation of a dmsnK1-K2 deletion mutant

The *dmsnK1-K2* deletion mutant in *S. niveiscabiei* ST1015 was created using plasmid pAMR4 that replaces the target genes with an apramycin (*aac(3)IV*) resistance cassette via double homologous recombination [33]. A 3-kb region upstream and downstream of the target genes was amplified (Table S3) with Herculase II Fusion DNA Polymerase (Agilent

Technologies), cloned into pCR-BluntII-TOPO (Invitrogen), and sent for sequence verification (Laragen Inc., Culver City, CA). The constructs were digested with *Mfe*I/*BamH*I and *Avr*II/*Hind*III (New England Biolabs) to release the upstream and downstream regions, respectively, which were then cloned into the pAMR4 vector [33]. The resulting pAMR4SnUD deletion construct (Table S1) was introduced into *E. coli* ET12567 harboring plasmid pUZ8002 [34] via heat shock and transferred from the transformed *E. coli* strain to *S. niveiscabiei* ST1015 via intergeneric conjugation. Exconjugants were recovered on Soy Flour Mannitol (SFM) medium [34] (30 mL) that was overlaid with nalidixic acid and apramycin after 24 h and tested for sensitivity to kanamycin on ISP-2 medium [34]. Verification of the correct deletion of the target genes was performed via Polymerase Chain Reaction (PCR) (Fig. S1) using the primers listed in Table S3.

2.6. Genetic complementation of the dmsnK1-K2 deletion mutant

A 6182-bp fragment covering the cluster from *dmsnK1* to *dmsnO1* was PCR-amplified with the primers MIL20 and MIL21 (Table S3). This amplicon was cloned into the *Xba*I site of plasmid pAU3-45-ermEp to generate pAU3-45-c*dmsn*. The plasmid pAU3-45-ermEp was generated by cloning the ermE promotor, amplified with primers imf33/imf158 from pIJ8641 [35], into the *BamH*I site of plasmid pAU3-45 [36]. Plasmid pAU3-45-c*dmsn* was introduced into three independently generated mutant strains of ST1015Δ*dmsnK1-K2* by intergeneric conjugation as described above. Exconjugants were recovered on SFM medium overlaid with nalidixic acid, thiostrepton and apramycin after 24 h of incubation at 28 °C [34]. One PCR-verified exconjugant colony from each complemented mutant background was randomly selected and used in the phenotypic assays. Because these complemented strains were derived from independent mutant backgrounds, biological replication in these experiments is defined at the strain level rather than the colony level.

2.7. Radish bioassays

Radish seedling assays were used to evaluate either the virulence capacity of the bacteria or the presence of phytotoxic compounds in the supernatant of bacterial cultures. Bacterial cells from a 24-h TSB culture (5 mL) were prepared as inoculum as previously described by Lapaz et al. [10]. To obtain culture supernatant, cells from TSB precultures, grown as described above, were pelleted by centrifugation, washed twice, and resuspended in one mL of sterile distilled water to an optical density at 600 nm (OD_{600nm}) of 1. Aliquots of 200 µL of these mycelial suspensions were used to inoculate 50 mL of TSB, Oat Bran Broth (OBB) [37]), Potato Mash Broth (PMB, 12.5 g dried potato flakes per liter), a broth based on the ingredients of ISP-4 medium (BD Biosciences, Franklin Lakes, NJ, USA) omitting the agar, and/or a broth based on the ingredients of ISP-2 medium (BD Biosciences, Franklin Lakes, NJ, USA) omitting the agar. Cultures were incubated for 1–7 days at 28 °C at 220 rpm. Cultures were centrifuged and their supernatant was filtered through 0.45 µm syringe filters. The filtrates were tested for phytotoxicity on radish seedlings (200 µL per germinated seed). Filtered uninoculated media were used as negative controls. Each treatment included 6 seedlings per replicate, and assays were repeated three times. Seedlings were grown at 24 ± 2 °C with a 16-h photoperiod for 7 days. After incubation, the shoot length of each seedling was measured, and values were expressed as ratios relative to the mean length of water-treated control seedlings. These normalized data were used for statistical comparison among treatments.

2.8. Potato disk bioassays

The phytotoxicity of culture supernatants was also evaluated using potato tuber disk assays. These assays were performed as described by Lapaz et al. [10] except that 25 µL culture supernatant was used as inoculum. Each treatment included five potato disks per replicate, and assays were performed three times independently. The wild-type strain ST1015 was included as a positive control, while water and uninoculated OBB medium [37] served as negative controls. After 5 days of incubation at 28 ± 2 °C in a humid chamber, lesion formation and tissue necrosis were evaluated qualitatively as the irregular shape and depth of lesions typically caused by *Streptomyces* species make accurate quantification of lesion area or severity index unreliable.

2.9. Detection of dmsn via HPLC analysis and confirmation by NMR spectroscopy

HPLC analysis was carried out following reverse-phase C18 methods previously established for aromatic type II polyketides from *Streptomyces* [38] and subsequently adapted for dmsn detection in culture supernatants [39]. Samples of 10 mL of filtered supernatant, prepared as described above, were lyophilized and resuspended in 1.5 mL of methanol. HPLC analysis was performed on a Shimadzu Prominence LC-20AT equipped with an SPD-M20A diode-array detector using a SUPELCO discovery C18 column (4.6 × 150 mm, 5 µm particle size), maintained at room temperature. The gradient profile consisted of solvent A (acetic acid 0.5 % v/v) and solvent B (acetic acid 0.5 % v/v in acetonitrile). An initial hold (6 min, 20 % B) was followed by a linear gradient (30 % B after 7 min, 60 % B after 16 min, 90 % B after 22 min, 20 % B after 27 min) and held at 20 % B for an additional 13 min. The solvent flow was 0.5 mL/min and samples were monitored at 254 nm. Desmethylmensacarcin was identified by comparison of its retention time to that of the purified compound [19].

The presence or absence of dmsn in the supernatant was also confirmed through NMR spectroscopy. 10 mL samples of the filtered supernatant, prepared as described above, were lyophilized, resuspended in 600 µL of D_2O, and transferred to 5 mm NMR tubes (NE HL5 7, New Era Enterprises, Vineland, NJ, USA). Water-suppressed ^1H NMR spectra were recorded on a Bruker AVANCE III 500 spectrometer operating at a ^1H frequency of 500.13 MHz using previously described parameters and conditions. The presence of dmsn in the supernatants was confirmed by identification of several of the characteristic ^1H NMR signals of the phytotoxin previously assigned on a purified sample [19].

2.10. Statistical analysis

For radish seedling assays, phytotoxicity was quantified based on the ratio of shoot length relative to the mean shoot length of seedlings treated with water, which served as the reference control. Data from three independent experiments ($n = 3$), each including six seedlings per treatment, were analyzed using one-way analysis of variance (ANOVA) followed by Tukey's post hoc test ($\alpha = 0.05$). Differences among treatments were considered statistically significant at $p < 0.05$ and highly significant when $p < 0.001$. Statistical analyses and boxplots were generated using Python 3.10.

3. Results

3.1. Production of dmsn in plant-based media

The production of phytotoxic compounds in 7-day old supernatants from different culture media was evaluated via radish seedling assays. Phytotoxicity was quantified as the shoot-length ratio relative to water-treated controls revealing highly significant differences among media (one-way ANOVA, $F(4,10) = 79.03$, $p = 1.58 \times 10^{-7}$, $n = 3$; Table S4). Seedlings treated with cell-free supernatants from OBB and PMB cultures showed marked growth inhibition and root necrosis, while no phytotoxicity was detected in seedlings treated with supernatants from TSB, ISP-2, or ISP-4 cultures (Fig. 1). Phytotoxicity of the OBB and PMB culture supernatants was generally observed starting at two days post inoculation (Fig. S2). Moreover, the presence of dmsn in the OBB culture

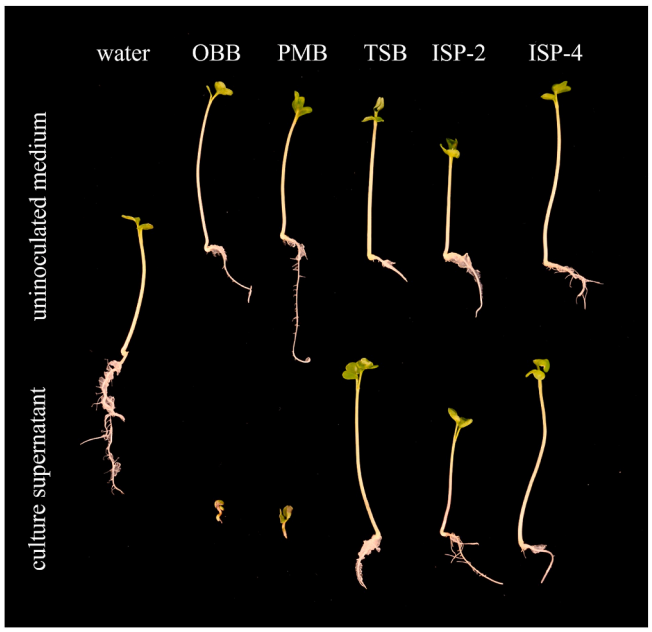

Fig. 1. Radish assay to assess the phytotoxicity of the supernatant of the wild type *Streptomyces niveiscabiei* ST1015 cultures. Germinated seeds were inoculated with 200 µL of water or cell-free supernatant of cultures grown for 3 days in OBB, PMB, TSB, ISP-2, and ISP-4. The phenotype of a representative radish seedling for each treatment is shown at 7 days post inoculation.

supernatant and the absence of dmsn in the TSB supernatant was further supported by chemical analysis. HPLC analysis of culture supernatants collected at 1, 2, 3, 5, and 7 days post inoculation (dpi) revealed a consistent retention time matching that of the purified dmsn standard (Fig. S3) in both OBB and PMB media, starting as early as 2 dpi (Fig. S4). No dmsn peak was detected in the supernatants from TSB cultures at any time point (Fig. S4). In parallel, time-course ^{1}H NMR analysis confirmed the appearance of dmsn-characteristic signals in OBB supernatants beginning at 3 dpi. In particular, resonances corresponding to the H-6, H-7, and H-8 protons on the aromatic ring, H-4, H-10, H-12, and H-13 protons sitting on oxygen-bearing carbons, and CH_3-14 and CH_3-15 methyl protons can be unambiguously identified (Fig. S5). On the other hand, these signals remained absent in TSB supernatants throughout the 7-day period (Fig. S6). These results show that dmsn was detected only in plant-based media and that its presence coincides with the phytotoxic activity of culture supernatants.

3.2. *S. niveiscabiei ST1015 contains a 22-gene cluster with strong homology to the msn BGC of S. bottropensis Gö C4/4*

The newly generated complete genome of *S. niveiscabiei* ST1015 was analyzed to identify the BGC responsible for the production of the phytotoxic polyketide dmsn, shown to cause deep pitted necrotic lesions on potato tubers [19].

AntiSMASH analysis revealed a total of 41 putative secondary metabolite clusters, including a gene cluster (cluster 40) with 84 % homology to the msn biosynthetic cluster of *S. bottropensis* Gö C4/4 (Table 1). Several other biosynthetic clusters were predicted with high confidence (>80 % similarity) and code for the siderophores coelichelin and desferrioxamine B [40,41], the antimicrobial compounds albaflavenone and nikkomycin [42,43], the osmolyte ectoine [44], a gamma-butyrolactone signaling molecule generally regulating antibiotic production and differentiation in *Streptomyces* [45], and the hopanoid hopene involved in controlling membrane fluidity and diminishing passive diffusion of ions through the cell membrane [44] (Table 1).

Cluster 40 represents the dmsn cluster of *S. niveiscabiei* ST1015 and contains 22 open reading frames (*orfs*). All are homologs to corresponding genes of the msn cluster of *S. bottropensis* Gö C4/4 (Table 2). Moreover, gene order and orientation are conserved among the two clusters. The ST1015 dmsn cluster contains genes coding for three proteins of the minimum PKS system (two ketosynthases and an acyl carrier protein), five reductases, six oxygenases, three cyclases, two regulators of which one belongs to the *Streptomyces* antibiotic regulatory protein (SARP) family [46], a transporter of the major facilitator superfamily (MFS), a NAD(P)H binding protein, a phophotransferase, and an α/β-fold hydrolase. Consistent with the dmsn chemical structure [19], the three genes involved in methylation of msn, *msnM1*, *msnM2* and *msnM3,* were not found in the dmsn cluster of ST1015 (Table 2).

3.3. *The dmsn cluster is also present in other Streptomyces species*

To explore the diversity and distribution of BGCs encoding the thaxtomin and msn/dmsn biosynthetic pathways, a similarity network analysis was performed using BiG-SCAPE [31]. Three distinct GCFs were identified, each grouping BGCs with high sequence similarity (Fig. 2). Two GCFs corresponded to thaxtomin-like BGCs. The largest GCF, centered around the MiBIG reference cluster BGC00002089, grouped BGCs from multiple *Streptomyces* species, with *S. scabiei* (pink nodes) being predominant. This cluster showed high conservation, with strong connectivity among members, suggesting a widespread and conserved distribution of the thaxtomin biosynthetic capability among pathogenic *Streptomyces* species. In addition, a smaller GCF included BGC0000444 and consisted of more divergent clusters from *S. turgidiscabies* strains (brown nodes). The third GCF was associated with msn/dmsn biosynthesis. This family included the previously characterized msn BGC from *S. bottropensis* (yellow node). Additionally, closely related BGCs from *S. acidiscabies* (green nodes) and *S. niveiscabiei* (orange nodes) were included, suggesting a broader distribution of msn/dmsn-like biosynthetic capabilities within the *Streptomyces* genus than previously recognized.

To further investigate the genetic architecture of the BGCs grouped within the msn/dmsn-associated GCF, we performed a synteny comparison of representative clusters using Cagecat (Fig. 3). The BGC from *S. bottropensis* Gö C4/4, previously associated with the biosynthesis of msn, served as a reference. The analysis revealed a high degree of gene conservation and synteny among BGCs from *S. bottropensis*, *S. acidiscabies*, and *S. niveiscabiei*, with the main polyketide synthase and tailoring genes consistently present across all strains. As previously noted for *S. niveiscabiei* ST1015, the *msnM1–M3* genes were also absent in the BGCs of other *S. niveiscabiei* strains as well as for *S. acidiscabies*.

3.4. *Linking genomic variation in dmsn BGCs to phytotoxin production*

Previous work by Croce et al. [39] demonstrated that among the sequenced *S. niveiscabiei* strains, only ST1015 was able to produce dmsn in culture supernatant, while ST1020 did not. Regarding the species *S. acidiscabies,* none of the strains tested were found to produce this metabolite. In this study, we used comparative genomic analysis to examine whether differences in BGC structure or sequence content among these strains could account for the observed variation in dmsn production.

Most of the genes comprising the dmsn BGC are highly similar between *S. niveiscabiei* strains ST1015 and ST1020. However, three genes (*dmsnO2*, *dmsnK2*, and *dmsnO11*) showed lower sequence homology (Fig. 3). Further sequence alignment (Fig. S7) revealed the presence of premature stop codons in these three genes in the ST1020 strain. In particular, the *dmsnK2* gene, which encodes a core biosynthetic enzyme, contains a premature stop codon followed immediately by an alternative start codon (GTG) (Fig. S7A). This arrangement could potentially lead to the translation of a truncated protein consisting of only 116 amino acids of which the functionality is uncertain. In contrast, the absence of dmsn

Table 1
Putative secondary metabolite clusters on the *Streptomyces niveiscabiei* ST1015 genome predicted by AntiSMASH 7.0

Region	Type	From	To	Most similar known cluster	Type	Similarity
1	redox cofactor	74,362	96,507	dutomycin	Polyketide	4 %
2	T2PKS	142,404	214,582	rabelomycin/dehydrorabelomycin/fluostatin F/ fluostatin G/fluostatin H	Polyketide: Type II	18 %
3	phosphonate, trans AT-PKS, NRPS, NRPS-like	344,877	462,562	phthoxazolin	NRP + Polyketide	11 %
4	terpene	669,651	689,999	ebelactone	Polyketide	5 %
5	T3PKS, terpene, other	734,773	781,541	furaquinocin B	Terpene + Polyketide	34 %
6	NRPS	810,554	863,009	coelibactin	NRP	72 %
7	NRPS	938,492	988,337	coelichelin	NRP	90 %
8	terpene	1,013,386	1,033,532			
9	T1PKS, furan	1,058,203	1,101,528	glycinocin A	NRP	6 %
10	terpene, indole	1,103,529	1,127,659	A-503083 A/A-503083 B/A-503083 E/A-503083 F	NRP	5 %
11	NRPS	1,235,383	1,293,229	friulimicin A/friulimicin B/friulimicin C/friulimicin D	NRP	12 %
12	butyrolactone	1,306,227	1,316,776	streptovaricin	Polyketide	7 %
13	amglyccycl, NRPS, hglE-KS, T1PKS	1,343,770	1,433,830	thiazostatin/watasemycin A/watasemycin B/2-hydroxy phenylthiazoline enantiopyochelin/isopyochelin	NRP	33 %
14	terpene	1,492,310	1,516,345	hopene	Terpene	92 %
15	NRPS	1,576,141	1,640,368	atratumycin	NRP	7 %
16	indole	1,710,042	1,731,190	5-isoprenylindole-3-carboxylate β-D-glycosyl ester	Other	23 %
17	NRPS, β-lactone	1,878,330	1,981,118	malacidin A/malacidin B	NRP: Ca + -dependent lipopeptide	30 %
18	siderophore	1,999,189	2,012,072	grincamycin	Polyketide: Type II + Saccharide: Hybrid/tailoring	8 %
19	NRPS-like, β-lactone, nucleoside	2,028,572	2,077,007	neopolyoxin C	Other	100 %
20	terpene, butyrolactone	2,229,653	2,250,513	γ-butyrolactone	Other	100 %
21	RiPP-like	2,299,460	2,309,759			
22	T2PKS	2,382,865	2,454,250	xantholipin	Polyketide	67 %
23	siderophore	2,566,885	2,578,727			
24	NRPS, NRPS-like	2,960,713	3,021,844	cysteoamide	NRP	63 %
25	terpene	3,303,019	3,323,372	albaflavenone	Terpene	100 %
26	lanthipeptide-class-iii	4,752,896	4,774,163			
27	siderophore	6,031,576	6,042,528	desferrioxamine B/desferrioxamine E	Other	83 %
28	melanin	6,152,059	6,162,475	lactonamycin	Polyketide	10 %
29	RRE-containing	6,206,144	6,227,271			
30	NAPAA	7,425,419	7,459,261			
31	T3PKS	7,997,439	8,038,488	herboxidiene	Polyketide	7 %
32	other, NRPS, NRPS-like, T1PKS, T2PKS	8,201,856	8,376,149	kedarcidin	Polyketide: Iterative type I + Polyketide: Enediyne type I	5 %
33	RiPP-like, lanthipeptide-class-iii	8,659,633	8,687,302	informatipeptin	RiPP: Lanthipeptide	100 %
34	siderophore	8,688,946	8,703,410			
35	T1PKS	9,021,796	9,064,533	jawsamycin	NRP + Polyketide	23 %
36	guanidinotides	9,193,321	9,216,906	glycopeptidolipid	NRP	20 %
37	T1PKS, ectoine	9,283,888	9,326,831	ectoine	Other	100 %
38	NRPS-like, T1PKS	9,460,534	9,505,296	meridamycin	NRP + Polyketide	10 %
39	arylpolyene, T1PKS, PKS-like, NRPS	9,676,597	9,772,104	7-deoxypactamycin	Polyketide: Iterative type I + Saccharide: Hybrid/tailoring	41 %
40	T2PKS	9,855,512	9,928,021	mensacarcin	Polyketide: Type II	84 %
41	terpene	10,135,630	10,157,285			

detection in *S. acidiscabies* strains cannot be explained by the loss of specific biosynthetic genes or by disruptive mutations such as premature stop codons. However, as shown in Fig. 3, the *dmsnR2* gene, a putative regulatory gene, appears highly conserved within *S. acidiscabies* strains but not when compared with *S. niveiscabiei* strains (Fig. S7D).

3.5. Deletion of dmsnK1-K2 abolishes the production of dmsn

To link the production of the phytotoxin dmsn to the identified PKS cluster and to evaluate its importance in the infection process of the bacterium, a deletion mutant was created exchanging the region spanning two central genes in the biosynthetic cluster, the ketosynthase genes *dmsnK1* and *dmsnK2*, for an apramycin (*aac(3)IV*) resistance cassette carried on the plasmid pAMR4 [33].

Three independently generated mutant isolates were evaluated for their ability to cause root and shoot stunting of radish seedlings. When seedlings were inoculated with live bacterial cultures, all three Δ*dmsnK1–K2* mutants induced stunting comparable to the wild-type strain ST1015, with no statistically significant differences among treatments (one-way ANOVA, $F(3,8) = 1.07$, $p = 0.41$, n = 3; Table S5 and Fig. 4A). However, when performing these same bioassays using the supernatant of OBB cultures from both wild type and mutant strains, the deletion of the ketosynthase genes (*dmsnK1–K2*) completely abolished the phytotoxicity effect. Quantitative analysis of phytotoxicity revealed highly significant differences among treatments (one-way ANOVA, $F(4,10) = 46.20$, $p = 2.0 \times 10^{-6}$, $n = 3$). Seedlings treated with wild-type supernatant showed a marked reduction in shoot length ratios (0.10 ± 0.04), whereas those treated with culture supernatants from any of the mutant strains showed normal growth, with ratios similar to the uninoculated OBB medium (0.846 ± 0.08) (Fig. 4B–Table S5). Complementation of each Δ*dmsnK1–K2* mutant with the plasmid pAU3-45-c*dmsn*, restored the phytotoxicity of the culture supernatant as seen by the severe stunting of radish seedling growth and necrosis on potato tuber disks (Fig. 5). Quantitative analysis of seedling shoot length ratios confirmed that shoot lenghts of seedlings inoculated with culture supernatant of the complemented strains did not differ significantly from those inoculated with culture supernatant of the wild type, while both showed a strong reduction compared to seedlings inoculated with the

Table 2
Comparison of the mensacarcin gene cluster of *Streptomyces bottropensis* Gö C4/4 with the complete genome of *Streptomyces niveiscabiei* ST1015.

***S. bottropensis* Gö C4/4 msn gene cluster (KJ437437)**		**Predicted *S. niveiscabiei* ST1015 dmsn biosynthetic gene cluster**		**% Identity**	**% Coverage**	**E-value**
Protein id	**Gene***	**Predicted gene**	**Predicted protein product**			
AHL46681.1	*msnO1*	*A7X85_01230*	Ketoreductase	86.07	98	$3e^{-164}$
AHL46682.1	*msnO2*	*A7X85_01235*	Luciferase-like monooxygenase	88.32	100	0.0
AHL46683.1	*msnO3*	*A7X85_01240*	Flavin reductase	76.30	100	$2e^{-98}$
AHL46684.1	*msnH5*	*A7X85_01245*	Phosphotransferase family protein	73.67	97	$9e^{-179}$
AHL46685.1	*msnK2*	*A7X85_01250*	Ketosynthase	88.92	99	0.0
AHL46686.1	*msnK1*	*A7X85_01255*	Ketosynthase	94.76	99	0.0
AHL46687.1	*msnH6*	*A7X85_01260*	NAD(P)H binding protein	75.72	98	$6e^{-141}$
AHL46688.1	*msnO4*	*A7X85_01265*	Luciferase-like monooxygenase	85.52	100	0.0
AHL46689.1	*msnO5*	*A7X85_01270*	Monooxygenase	80.20	100	$6e^{-64}$
AHL46690.1	*msnC1*	*A7X85_01275*	Putative bifunctional cyclase/dehydratase	70.12	100	0.0
AHL46691.1	*msnO6*	*A7X85_01280*	Monooxygenase	74.29	100	$2e^{-59}$
AHL46692.1	*msnO7*	*A7X85_01285*	Monooxygenase	85.29	98	$4e^{-66}$
AHL46693.1	*msnC2*	*A7X85_01290*	Putative cyclase	84.18	96	0.0
AHL46694.1	*msnO8*	*A7X85_01295*	Luciferase-like monooxygenase	88.62	100	0.0
AHL46695.1	*msnO9*	*A7X85_01300*	Putative NADPH:quinone oxidoreductase	84.83	100	0.0
AHL46696.1	*msnO10*	*A7X85_01305*	Ketoreductase	79.62	100	$8e^{-146}$
AHL46697.1	*msnK3*	*A7X85_01310*	Acyl carrier protein	84.88	87	$1e^{-53}$
AHL46698.1	*msnO11*	*A7X85_01315*	Ketoreductase	87.36	100	$9e^{-173}$
AHL46699.1	*msnC3*	*A7X85_01320*	Putative bifunctional cyclase/dehydratase	81.53	100	0.0
AHL46700.1	*msnR1*	*A7X85_01325*	SARP regulatory protein	74.81	93	$6e^{-148}$
AHL46701.1	*msnH7*	*A7X85_01330*	Alpha/beta fold hydrolase	69.00	99	$3e^{-141}$
AHL46702.1	*msnH8*	*A7X85_01335*	MSF transporter	18.75	23	$2e^{-58}$
AHL46703.1	*msnR2*	*A7X85_01340*	Regulatory protein	53.42	99	0.0
AHL46704.1	*msnM1*	Not present	Adenosylhomocysteinase	/	/	/
AHL46705.1	*msnM2*	Not present	N5,N10-methylenetetrahydrofolate reductase	/	/	/
AHL46706.1	*msnM3*	Not present	Methionine synthase	/	/	/

* The color code refers to the colors used in Figure 3.

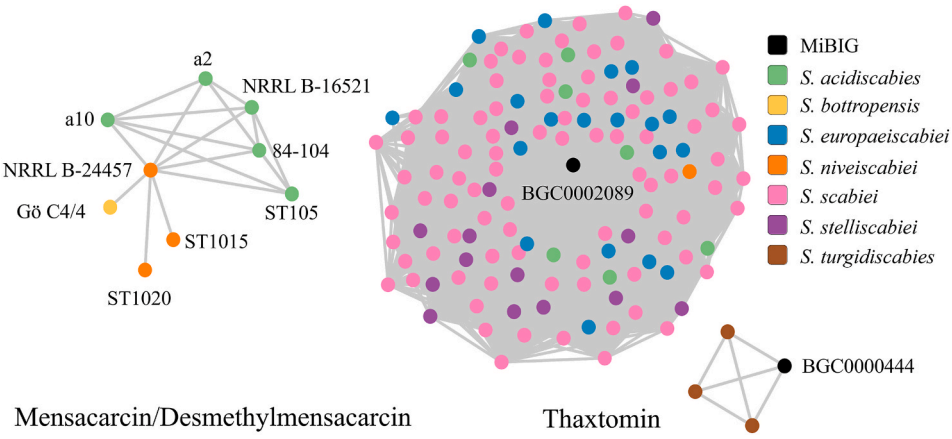

Fig. 2. Distribution of biosynthetic gene clusters (BGCs) encoding the thaxtomin and mensacarcin/desmethylmensacarcin biosynthetic pathways within representative *Streptomyces* strains. Nodes represent individual BGCs and are color-coded according to their species as shown in the legend. Black nodes correspond to BGCs from MiBIG database. Edges connect clusters with domain similarity above the sequence similarity cutoff (0.3). Analysis was performed using BiG-SCAPE (version 1.1.5). (For interpretation of the references to color in this figure legend, the reader is referred to the Web version of this article.)

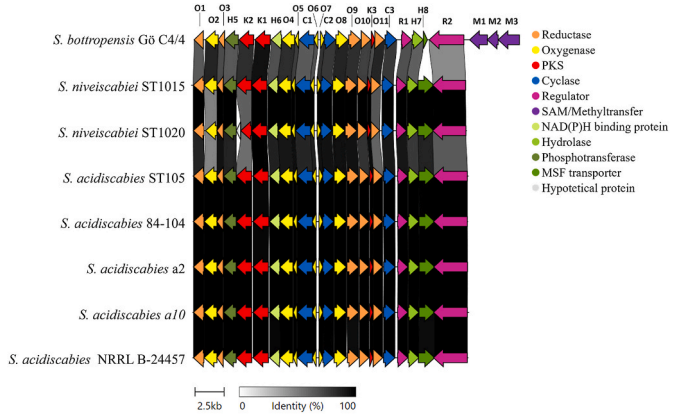

Fig. 3. Synteny comparison of mensacarcin/desmethylmensacarcin biosynthetic gene clusters (BGCs) among pathogenic *Streptomyces* species. Colored arrows represent individual genes within the cluster, drawn to scale. Each arrow indicates the direction of transcription and is color-coded according to gene function as shown in the legend. Homologous genes identified across related clusters are connected by gray shading, with darker shades indicating higher sequence identity (>80 %). The BGC from *S. bottropensis* Gö C4/4 is shown as reference with gene names indicated above each arrow. The scale bar corresponds to 2.5 kb. (For interpretation of the references to color in this figure legend, the reader is referred to the Web version of this article.)

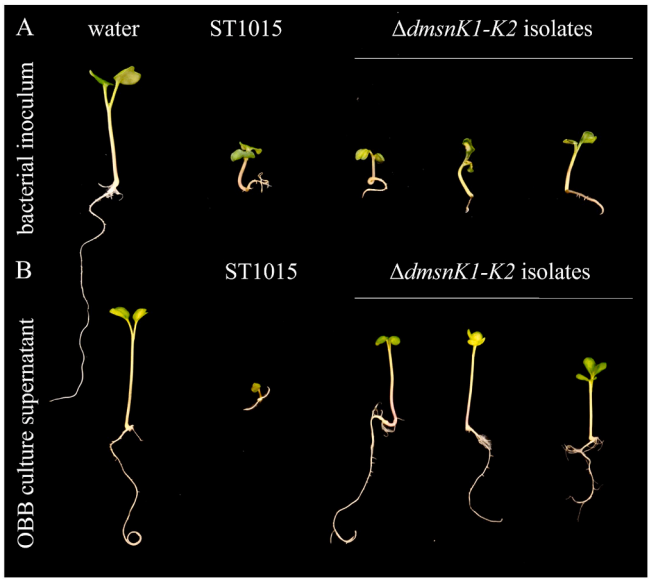

Fig. 4. Radish assay to assess the phytotoxicity of the wild type *Streptomyces niveiscabiei* ST1015Δ*dmsnK1-K2* mutant isolates. Germinated seeds were inoculated with 200 μL of either a washed bacterial suspension set to OD_{600} 1.0 of the wild type ST1015 and three independently generated ST1015Δ*dmsnK1-K2* isolates (A) or cell-free supernatant of cultures of ST1015 and the ST1015Δ*dmsnK1-K2* isolates grown in OBB for 5 days (B). Water was used as the negative control. The phenotype of a representative radish seedling for each treatment is shown at 7 days post inoculation.

mutant isolates and the mock inoculated control treatment (one-way ANOVA, $F(4,10) = 89.81$, $p = 8.5 \times 10^{-8}$, $n = 3$; Fig. 6).

To confirm the presence or absence of dmsn in the respective supernatants, the ^{1}H NMR metabolic profiles of the OBB culture supernatant of the mutant strains were compared to the ones of the ST1015 wild type and uninoculated OBB medium. Stacked ^{1}H NMR spectra with the signals that are characteristic for dmsn are shown in Fig. 6. These resonances were absent in the spectra of uninoculated OBB or the OBB culture supernatant of the six mutant strains that were evaluated for this assay (Fig. 7).

4. Discussion

Desmethylmensacarcin (dmsn) is a polyketide structurally related to msn, which was originally isolated from *Streptomyces bottropensis* and displays antitumor activity [21]. More recently, dmsn was identified in *Streptomyces niveiscabiei* ST1015 and shown to act as a phytotoxin involved in plant tissue damage during common scab disease [19]. In this work, we identified and functionally validated the BGC responsible for dmsn production, expanding the current understanding of secondary metabolites involved in potato common scab pathogenesis.

Our findings indicated that dmsn biosynthesis is strongly influenced by the growth environment, being activated only under plant-based culture conditions. This pattern suggests that dmsn production is regulated by specific nutritional or plant-derived cues rather than by general metabolic activity. This early and media-specific activation is consistent with reports showing that the expression of many BGCs in *Streptomyces* is often modulated by nutrient availability, stress, or plant-derived signals [47,48]. A similar phenomenon has been described for thaxtomin A, the primary phytotoxin produced by several pathogenic *Streptomyces* species, including *S. scabiei*, where its biosynthesis is induced in the presence of cello-oligosaccharides such as cellobiose and cellotriose, as well

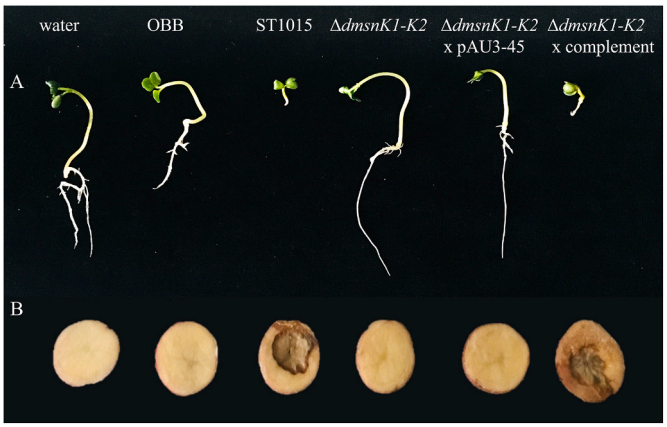

Fig. 5. Radish assay (A) and potato tuber disk assay (B) to assess the phytotoxicity of the supernatant of cultures of the wild type *Streptomyces niveiscabiei* ST1015, three independently generated ST1015 Δ*dmsnK1-K2* mutant isolates and their respective complemented strains ST1015 Δ*dmsnK1-K2* x complement. Germinated seeds and sterile potato tuber disks were inoculated with respectively 200 µL and 25 µL of cell-free bacterial supernatant of 5-day old OBB cultures. Water and non-inoculated OBB were used as negative controls. Phenotypes of a representative radish seedling or potato tuber disk are shown for each treatment at respectively 7- and 10-days post inoculation.

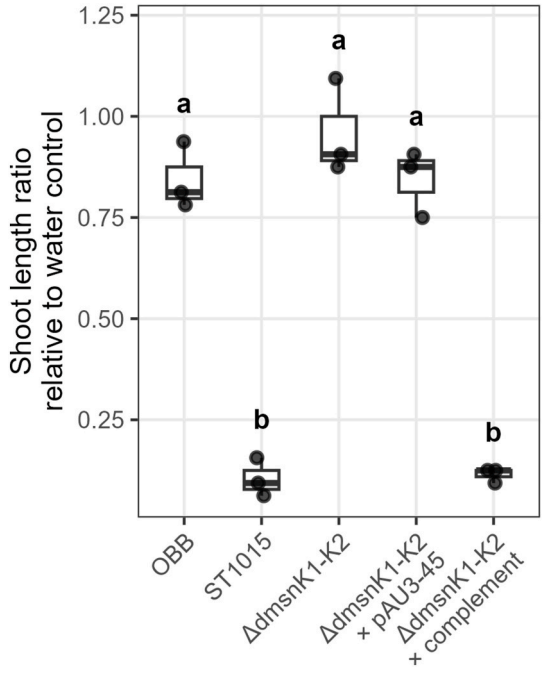

Fig. 6. Quantitative analysis of the phytotoxicity of culture supernatants from wild-type, mutant, and complemented strains. Shoot length ratios of radish seedlings treated with 200 µL of cell-free culture supernatants from the wild-type strain *Streptomyces niveiscabiei* ST1015, three independently generated ST1015 Δ*dmsnK1–K2* mutant isolates, the respective negative vector control strains (ST1015 Δ*dmsnK1–K2* × pAU3-45), and the complemented mutants (ST1015 Δ*dmsnK1–K2* × complement). Uninoculated OBB medium served as the negative control. Ratios were calculated relative to the mean shoot length of seedlings treated with water. Each point represents one biological replicate ($n = 3$ independent experiments). Boxplots show the mediant, interquartile range, and data distribution. Different letters indicate statistically significant differences among treatments (one-way ANOVA followed by Tukey's test, $p < 0.05$).

as suberin, a key component of the potato periderm [49,50].

Comparative genomic analysis revealed that the dmsn gene cluster in *S. niveiscabiei* ST1015 is highly syntenic to the msn cluster from

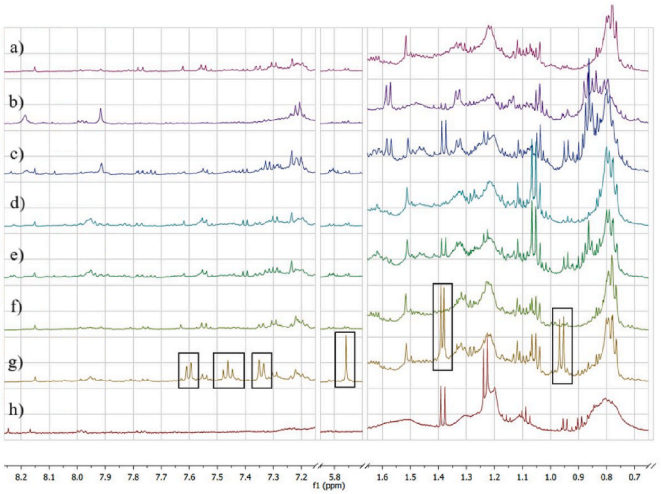

Fig. 7. Stacked ^{1}H NMR spectra of 7-day old OBB culture supernatants from six independently generated *Streptomyces niveiscabiei* ST1015 Δ*dmsnK1-K2* mutant isolates (a–f), the wild type strain ST1015 (g), and uninoculated OBB medium used as a negative control (h). Spectral regions above 8.3 ppm, between 7.1–5.9 and 1.7–5.6 ppm, and below 0.6 ppm contained no relevant signals and are not shown. Characteristic desmethylmensacarcin (dmsn) signals (boxed) corresponding to the ^{1}H NMR signals from aromatic H-6, H7, and H-8 protons, the H-10 proton, and the CH_3-14 and CH_3-15 methyl protons are visible in the wild-type supernatant and absent from all the mutants and control samples. A complete assignment of the dmsn ^{1}H NMR signals observed in the wild type ST1015 OBB culture supernatant is provided in Fig. S5.

S. bottropensis Gö C4/4, with the absence of the three methyltransferase genes (*msnM1-M3*) explaining the structural difference between dmsn and msn. This finding reinforces previous chemical evidence that dmsn is the final product of the pathway in ST1015 [19]. The presence of similar dmsn-like clusters in *S. niveiscabiei* ST1020 and *S. acidiscabies* strains, further indicates that this BGC family is more widely distributed among phytopathogenic *Streptomyces* strains than previously recognized. BiG-SCAPE analysis revealed that while thaxtomin clusters are broadly conserved and widely distributed among pathogenic *Streptomyces* species, msn/dmsn-type clusters appear more restricted in occurrence and associated with select lineages. The co-occurrence of these functionally distinct phytotoxic BGCs within a single genome, as observed in *S. niveiscabiei* NRRL B-24457 and few *S. acidiscabies* strains, is consistent with previous reports showing that *Streptomyces* species can harbor multiple toxin biosynthetic pathways that are differentially expressed and associated with specific roles during host colonization [48,51–53].

Interestingly, genetic variation within the dmsn cluster appears to underlie the contrasting metabolite production profiles observed among *S. niveiscabiei* and *S. acidiscabies* strains. In ST1020 potentially inactivating mutations, such as premature stop codons in key biosynthetic genes (e.g., *dmsnK2*), likely inactivate the pathway explaining the lack of dmsn production. In contrast, no obvious disruptions were found in the *S. acidiscabies* clusters, although divergence in regulatory sequences, particularly in *dmsnR2*, might underline the silencing of the pathway under the conditions tested. This highlights how even subtle variations in biosynthetic or regulatory architecture can result in significant phenotypic differences, a phenomenon that has been increasingly recognized through large-scale comparative analyses of natural product gene clusters [54,55]. Similar observations have been reported in *Streptomyces venezuelae*, where a single base deletion in the *cmlI* gene of the chloramphenicol BGC renders one strain incapable of producing the antibiotic, while closely related strains remain fully functional [56].

Functional assays provide direct evidence linking the dmsn BGC to the production of phytotoxin. Deletion of the core ketosynthase genes (*dmsnK1–K2*) completely abolished dmsn biosynthesis while genetic

complementation restored both metabolite production and phytotoxicity, as confirmed by quantitative radish seedling assays. This pattern parallels previous functional studies in *Streptomyces scabiei* and *S. turgidiscabies*, where disruption of thaxtomin biosynthetic genes similarly eliminated virulence-associated toxicity [49,50]. Despite the potent bioactivity of dmsn and its ability to mimic thaxtomin A–like necrosis in tuber disks and seedling assays [19], the virulence phenotype of the deletion mutant did not differ markedly from the wild type *in planta*. This unexpected result suggests that dmsn is not the sole virulence determinant in ST1015. The persistence of pathogenicity in the absence of dmsn production points to additional, yet unidentified, virulence factors that may act redundantly or synergistically. This is consistent with findings in other phytopathogenic *Streptomyces* species, where virulence is known to be multifactorial [57]. Recent studies have shown that, beyond thaxtomin A, *S. scabiei* and related species can produce a variety of other virulence-associated metabolites whose presence and regulation contribute significantly to disease severity [52]. This interpretation aligns with a recent population-scale genomic surveys of *Streptomyces* causing potato common scab, which revealed high genetic and species diversity and showed that virulence level correlates with the combined presence of multiple virulence-associated clusters rather than a single determinant [56].

While this study identifies and validates the dmsn BGC, further work is needed to determine the environmental signals regulating its activation and to quantify its contribution to disease under field conditions. Future studies combining transcriptomics and metabolomics will be crucial to elucidate how dmsn interacts with other virulence determinants and contributes to host specificity.

Overall, our findings expand the current understanding of the genetic and ecological diversity of phytotoxic metabolites in pathogenic *Streptomyces*, highlighting the value of integrative approaches that combine genomic, chemical, and phenotypic data to uncover novel virulence factors and their regulation.

CRediT authorship contribution statement

María Inés Lapaz: Writing – original draft, Visualization, Validation, Methodology, Investigation, Conceptualization. **Sofia Zeballos-Gorón:** Writing – review & editing, Visualization, Investigation, Data curation. **Valentina Croce:** Writing – review & editing, Investigation. **José Carlos Huguet-Tapía:** Software, Investigation, Data curation. **Martín Pérez-Baldassari:** Writing – review & editing, Investigation. **Andrés López:** Investigation. **Donald Hudson:** Investigation. **Sarah Forester:** Methodology, Investigation. **Rosemary Loria:** Supervision, Resources. **Guillermo Moyna:** Writing – review & editing, Methodology, Investigation. **María Julia Pianzzola:** Supervision, Resources, Methodology, Funding acquisition, Conceptualization. **María Inés Siri:** Writing – review & editing, Writing – original draft, Supervision, Resources, Methodology, Funding acquisition, Conceptualization. **Isolde M. Francis:** Writing – review & editing, Writing – original draft, Supervision, Resources, Methodology, Investigation, Funding acquisition, Conceptualization.

Funding sources

M.I.L. was supported by a doctoral grant from Comisión Académica de Posgrado (CAP-UdelaR). This work was also supported by the Comisión Sectorial de Investigación Científica (CSIC-UdelaR), the Centro de Estudios Interdisciplinarios de Biodiversidad Orientado a Aplicaciones en Salud (CEIBOS) funded by the Espacio Interdisciplinario (EI-UdelaR), and the Programa de Desarrollo de las Ciencias Básicas (PEDECIBA).

Glossary

(*continued on next column*)

(*continued*)

Abbreviation	Meaning
Abbreviation	Meaning
AntiSMASH	Antibiotics & Secondary Metabolite Analysis Shell
BGC	Biosynthetic Gene Cluster
CS	Common Scab
dpi	Days Post Inoculation
GCF	Gene Cluster Family
ISP	International *Streptomyces* Project
LB	Luria-Bertani
Mb	Megabase
MFS	Major Facilitator Superfamily
MiBIG	Minimum Information about a Biosynthetic Gene cluster
NCBI	National Center for Biotechnology Information
NMR	Nuclear Magnetic Resonance
NRPS	Non-Ribosomal Peptide Synthetase
OD600nm	Optical Density at 600 nm
OBB	Oat Bran Broth
ONT	Oxford Nanopore Technologies
ORF	Open Reading Frame
PCR	Polymerase Chain Reaction
PKS	Polyketide Synthase
PMB	Potato Mash Broth
RefSeq	Reference Sequence
SARP	*Streptomyces* Antibiotic Regulatory Protein
SFM	Soy Flour Mannitol
ST	Strain
TSB	Tryptic Soy Broth

Declaration of competing interest

The authors declare that they have no known competing financial interests or personal relationships that could have appeared to influence the work reported in this paper.

Acknowledgements

Plasmid pAMR4 was kindly provided by Dr. Jan Kormanec from the Slovak Academy of Sciences, Bratislava, Slovakia.

Appendix A. Supplementary data

Supplementary data to this article can be found online at https://doi.org/10.1016/j.pmpp.2025.103072.

Data availability

Data will be made available on request.

References

[1] M.W. Dees, L.A. Wanner, In search of better management of potato common scab, Potato Res. 55 (2012) 249–268, https://doi.org/10.1007/s11540-012-9206-9.
[2] K.F. Chater, S. Biró, K.J. Lee, T. Palmer, H. Schrempf, The complex extracellular biology of *Streptomyces*, FEMS Microbiol. Rev. 34 (2010) 171–198, https://doi.org/10.1111/j.1574-6976.2009.00206.x.
[3] R. Loria, D.R.D. Bignell, S. Moll, J.C. Huguet-Tapia, M.V. Joshi, E.G. Johnson, R. F. Seipke, D.M. Gibson, Thaxtomin biosynthesis: the path to plant pathogenicity in the genus *Streptomyces*, Antonie Leeuwenhoek 94 (2008), https://doi.org/10.1007/s10482-008-9240-4, 3-1.
[4] D. Guan, B.L. Grau, C.A. Clark, C.M. Taylor, R. Loria, G.S. Pettis, Evidence that thaxtomin C is a pathogenicity determinant of *Streptomyces ipomoeae*, the causative agent of *Streptomyces* soil rot of sweet potato, Mol. Plant Microbe Interact. 25 (2012) 393–401, https://doi.org/10.1094/MPMI-03-11-0073.
[5] R.R. King, L.A. Calhoun, The thaxtomin phytotoxins: sources, synthesis, biosynthesis, biotransformation and biological activity, Phytochemistry 70 (2009) 833–841, https://doi.org/10.1016/j.phytochem.2009.04.013.
[6] S.M. Barry, J.A. Kers, E.G. Johnson, L. Song, P.R. Aston, B. Patel, S.B. Krasnoff, B. R. Crane, D.M. Gibson, R. Loria, G.L. Challis, Cytochrome P450-acatlyzed L-tryptophan nitration in thaxtomin phytotoxin biosynthesis, Nat. Chem. Biol. 8 (2012) 814–816, https://doi.org/10.1038/nchembio.1048.
[7] W.R. Scheible, B. Fry, A. Kochevenko, D. Schindelasch, L. Zimmerli, S. Somerville, R. Loria, C.R. Somerville, An *Arabidopsis* mutant resistant to thaxtomin A, a

cellulose synthesis inhibitor from *Streptomyces* species, Plant Cell 15 (2003) 1781–1794, https://doi.org/10.1105/tpc.013342.
[8] J.K. Fyans, L. Bown, D.R.D. Bignell, Isolation and characterization of plant-pathogenic *Streptomyces* species associated with common scab-infected potato tubers in Newfoundland, Phytopathology 106 (2016) 123–131, https://doi.org/10.1094/PHYTO-05-15-0125-R.
[9] E. Jordaan, J.E. van der Waals, *Streptomyces* species associated with common scab lesions of potatoes in South Africa, Eur. J. Plant Pathol. 144 (2016) 631–643, https://doi.org/10.1007/s10658-015-0801-x.
[10] M.I. Lapaz, J.C. Huguet-Tapia, M.I. Siri, E. Verdier, R. Loria, M.J. Pianzzola, Genotypic and phenotypic characterization of *Streptomyces* species causing potato common scab in Uruguay, Plant Dis. 101 (2017) 1362–1372, https://doi.org/10.1094/PDIS-09-16-1348-RE.
[11] D.R.D. Bignell, J.C. Huguet-Tapia, M.V. Joshi, G.S. Pettis, R. Loria, What does it take to be a plant pathogen: genomic insights from *Streptomyces* species, Antonie Leeuwenhoek 98 (2010) 179–194, https://doi.org/10.1007/s10482-010-9429-1.
[12] Z. Cao, G. Khodakaramian, K. Arakawa, H. Kinashi, Isolation of borrelidin as a phytotoxic compound from a potato pathogenic *Streptomyces* strain, Biosci. Biotechnol. Biochem. 76 (2012) 353–357, https://doi.org/10.1271/bbb.110799.
[13] J.K. Fyans, M.S. Altowairish, Y. Li, D.R.D. Bignell, Characterization of the coronatine-like phytotoxins produced by the common scab pathogen *Streptomyces scabies*, Mol. Plant Microbe Interact. 28 (2015) 443–454, https://doi.org/10.1094/MPMI-09-14-0255-R.
[14] M. Natsume, A. Nagagata, M. Aittamaa, N. Okaniwa, P. Somervuo, H.P. Fiedler, J. F. Kreuze, V.M. Rokka, H. Bång, H. Kawaide, J.P.T. Valkonen, Phytotoxin produced by the netted scab pathogen, *Streptomyces turgidiscabies* strain 65, isolated in Sweden, J. Gen. Plant Pathol. 84 (2018) 108–117, https://doi.org/10.1007/s10327-018-0765-8.
[15] D.H. Park, J.S. Kim, S.W. Kwon, C. Wilson, Y.M. Yu, J.H. Hur, C.K. Lim, *Streptomyces luridiscabiei* sp. Nov., *Streptomyces puniscabiei* sp. Nov. and *Streptomyces niveiscabiei* sp. Nov., which cause potato common scab disease in Korea, Int. J. Syst. Evol. Microbiol. 53 (2003) 2049–2054, https://doi.org/10.1099/ijs.0.02629-0.
[16] D.H. Park, Y.M. Yu, J.S. Kim, J.M. Cho, J.H. Hur, C.K. Lim, Characterization of streptomycetes causing potato common scab in Korea, Plant Dis. 87 (2003) 1290–1296, https://doi.org/10.1094/PDIS.2003.87.11.1290.
[17] J. Wu, J. Duan, J. Li, Z. Liu, Q. Sun, R. Zhang, U. Handique, First report of *Streptomyces niveiscabiei* causing potato common scab in Shanxi and Gansu, China, Plant Dis. 107 (2023) 4016, https://doi.org/10.1094/PDIS-06-23-1039-PDN.
[18] M.I. Lapaz, E. Verdier, M.J. Pianzzola, First report regarding potato scab caused by *Streptomyces acidiscabies* in Uruguay, Plant Dis. 96 (2012) 1064, https://doi.org/10.1094/PDIS-02-12-0203-PDN.
[19] M.I. Lapaz, A. Lopez, J.C. Huguet-Tapia, M.F. Pérez-Baldassari, C. Iglesias, R. Loria, G. Moyna, M.J. Pianzzola, Isolation and structural characterization of a non-diketopiperazine phytotoxic compound from a potato pathogenic *Streptomyces* strain, Nat. Prod. Res. 33 (2019) 2951–2957, https://doi.org/10.1080/14786419.2018.1511554.
[20] Y. Zhang, D.R.D. Bignell, R. Zuo, Q. Fan, J.C. Huguet-Tapia, Y. Ding, R. Loria, Promiscuous pathogenicity islands and phylogeny of pathogenic *Streptomyces* spp, Mol. Plant Microbe Interact. 29 (2016) 640–650, https://doi.org/10.1094/MPMI-04-16-0068-R.
[21] M. Arnold, CD-aktive Metabolite Aus Streptomyceten Sowie Untersuchung Der Biosyntheseleistungen Des Mensacarcin-Bildners *Streptomyces* Sp. Gö C4/4, Cuvillier Verlag, Göttingen, 2002. Doctoral thesis.
[22] B. Plitzko, E.N. Kaweesa, S. Loesgen, The natural product mensacarcin induces mitochondrial toxicity and apoptosis in melanoma cells, J. Biol. Chem. 292 (2017) 21102–21116, https://doi.org/10.1074/jbc.M116.774836.
[23] I.M. Francis, D. Bergin, B. Deflandre, S. Gupta, J.J.C. Salazar, R. Villagrana, N. Stulanovic, S. Ribeiro Monteiro, F. Kerff, R. Loria, S. Rigali, Role of the alternative elicitor transporters in the onset of plant host colonization by *Streptomyces scabiei* 87-22, Biology 12 (2023) 234, https://doi.org/10.3390/biology12020234.
[24] M. Jain, H.E. Olsen, B. Paten, M. Akeson, The Oxford Nanopore MinION: delivery of nanopore sequencing to the genomics community, Genome Biol. 17 (2016) 239, https://doi.org/10.1186/s13059-016-1103-0.
[25] S. Koren, B.P. Walenz, K. Berlin, J.R. Miller, N.H. Bergman, A.M. Phillippy, Canu: scalable and accurate long-read assembly via adaptive k-mer weighting and repeat separation, Genome Res. 27 (2017) 722–736, https://doi.org/10.1101/gr.215087.116.
[26] N.J. Loman, J. Quick, J.T. Simpson, A complete bacterial genome assembled de novo using only nanopore sequencing data, Nat. Methods 12 (2015) 733, https://doi.org/10.1038/nmeth.3444.
[27] B.J. Walker, T. Abeel, T. Shea, M. Priest, A. Abouelliel, S. Sakthikumar, C. A. Cuomo, Q. Zeng, J. Wortman, S.K. Young, A.M. Earl, Pilon: an integrated tool for comprehensive microbial variant detection and genome assembly improvement, PLoS One 9 (2014) e112963, https://doi.org/10.1371/journal.pone.0112963.
[28] M. Kolmogorov, J. Yuan, Y. Lin, P.A. Pevzner, Assembly of long, error-prone reads using repeat graphs, Nat. Biotechnol. 5 (2019) 540–546, https://doi.org/10.1038/s41587-019-0072-8.
[29] R.R. Wick, K.E. Holt, Polypolish: short-read polishing of long-read bacterial genome assemblies, PLoS Comput. Biol. 18 (2022) e1009802, https://doi.org/10.1371/journal.pcbi.1009802.
[30] K. Blin, S. Shaw, H.E. Augustijn, Z.L. Reitz, F. Biermann, M. Alanjary, A. Fetter, B. R. Terlouw, W.W. Metcalf, E.J.N. Helfrich, G.P. van Wezel, M.H. Medema, T. Weber, antiSMASH 7.0: new and improved predictions for detection, regulation, chemical structures and visualisation, Nucleic Acids Res. 51 (2023) W46–W50, https://doi.org/10.1093/nar/gkad344.
[31] J.C. Navarro-Muñoz, N. Selem-Mojica, M.W. Mullowney, S.A. Kautsar, J.H. Tryon, E.I. Parkinson, E.L.C. De Los Santos, M. Yeong, P. Cruz-Morales, S. Abubucker, A. Roeters, W. Lokhorst, A. Fernandez-Guerra, L.T. Dias Cappelini, A.W. Goering, R.J. Thomson, W.W. Metcalf, N.L. Kelleher, F. Barona-Gomez, M.H. Medema, A computational framework to explore large-scale biosynthetic diversity, Nat. Chem. Biol. 16 (2020) 60–68, https://doi.org/10.1038/s41589-019-0400-9.
[32] M. van den Belt, C. Gilchrist, T.J. Booth, Y.-H. Chooi, M.H. Medema, M. Alanjary, CAGECAT: the comparative gene Cluster Analysis Toolbox for rapid search and visualisation of homologous gene clusters, BMC Bioinf. 24 (2023) 181, https://doi.org/10.1186/s12859-023-05311-2.
[33] R. Knirschova, R. Novakova, E. Mingyar, C. Bekeova, D. Homerova, J. Kormanec, Utilization of a reporter system based on the blue pigment indigoidine biosynthetic gene *bpsA* for detection of promoter activity and deletion of genes in *Streptomyces*, J. Microbiol. Methods 113 (2015) 1–3, https://doi.org/10.1016/j.mimet.2015.03.017.
[34] B. Gust, G.L. Challis, K. Fowler, T. Kieser, K.F. Chater, PCR-targeted *Streptomyces* gene replacement identifies a protein domain needed for the biosynthesis of the sesquiterpene soil odor geosmin, Proc. Natl. Acad. Sci. USA. 100 (2003) 1541–1546, https://doi.org/10.1073/pnas.0337542100.
[35] S. Sun, G.H. Kelemen, J.M. Fernández-Abalos, M.J. Bibb, Green fluorescent protein as a reporter for spatial and temporal gene expression in *Streptomyces coelicolor* A3 (2), Microbiology 145 (1999) 2221–2227, https://doi.org/10.1099/00221287-145-9-2221.
[36] D.R.D. Bignell, K. Tahlan, K.R. Colvin, S.E. Jensen, B.K. Leskiw, Expression of *ccaR*, encoding the positive activator of cephamycin C and clavulanic acid production in *Streptomyces clavuligerus*, is dependent on *bldG*, Antimicrob. Agents Chemother. 49 (2005) 1529–1541, https://doi.org/10.1128/aac.49.4.1529-1541.2005.
[37] E.G. Johnson, M.V. Joshi, D.M. Gibson, R. Loria, Cello-oligosaccharides released from host plants induce pathogenicity in scab-causing *Streptomyces* species, Physiol. Mol. Plant Pathol. 71 (2007) 18–25, https://doi.org/10.1016/j.pmpp.2007.09.003.
[38] X. Yan, K. Probst, A. Linnenbrink, M. Arnold, T. Paululat, A. Zeeck, A. Bechthold, Cloning and heterologous expression of three type II PKS gene clusters from *Streptomyces bottropensis*, Chembiochem 13 (2012) 224–230, https://doi.org/10.1002/cbic.201100574.
[39] V. Croce, A. López-Radcenco, M.I. Lapaz, M.J. Pianzzola, G. Moyna, M.I. Siri, An integrative approach for the characterization of plant-pathogenic *Streptomyces* spp. strains based on metabolic, bioactivity, and phylogenetic analysis, Front. Microbiol. 12 (2021) 643792, https://doi.org/10.3389/fmicb.2021.643792.
[40] F. Barona-Gómez, S. Lautru, F.X. Francou, P. Leblond, J.L. Pernodet, G.L. Challis, Multiple biosynthetic and uptake systems mediate siderophore-dependent iron acquisition in *Streptomyces coelicolor* A3(2) and *Streptomyces ambofaciens* ATCC 23877, Microbiology 152 (2006) 3355–3366, https://doi.org/10.1099/mic.0.29161-0.
[41] S. Lautru, R.J. Deeth, L.M. Bailey, G.L. Challis, Discovery of a new peptide natural product by *Streptomyces coelicolor* genome mining, Nat. Chem. Biol. 1 (2005) 265–269, https://doi.org/10.1038/nchembio731.
[42] H. Gürtler, R. Pedersen, U. Anthoni, C. Christophersen, P.H. Nielsen, E.M. H. Wellington, C. Pedersen, K. Bock, Albaflavenone, a sesquiterpene ketone with a zizaene skeleton produced by a streptomycetes with a new rope morphology, J. Antibiot. (Tokyo) 47 (1994) 434–439, https://doi.org/10.7164/antibiotics.47.434.
[43] G. Liu, Y. Tian, H. Yang, H. Tan, A pathway-specific transcriptional regulatory gene for nikkomycin biosynthesis in *Streptomyces ansochromogenes* that also influences colony development, Mol. Microbiol. 55 (2005) 1855–1866, https://doi.org/10.1111/j.1365-2958.2005.04512.x.
[44] S. Kol, M.E. Merlo, R.A. Scheltema, M. de Vries, R.J. Vonk, N.A. Kikkert, L. Dijkhuizen, R. Breitling, E. Takano, Metabolomic characterization of the salt stress response in *Streptomyces coelicolor*, Appl. Environ. Microbiol. 76 (2010) 2574–2581, https://doi.org/10.1128/AEM.01992-09.
[45] E. Takano, ɣ-butyrolactones: *streptomyces* signaling molecules regulating antibiotic production and differentiation, Curr. Opin. Microbiol. 9 (2006) 287–294, https://doi.org/10.1016/j.mib.2006.04.003.
[46] J. Krause, I. Handayani, K. Blin, A. Kulik, Y. Mast, Disclosing the potential of the SARP-type regulator PapR2 for the activation of antibiotic gene clusters in streptomycetes, Front. Microbiol. 11 (2020) 225, https://doi.org/10.3389/fmicb.2020.00225.
[47] P. Rutledge, G. Challis, Discovery of microbial natural products by activation of silent biosynthetic gene clusters, Nat. Rev. Microbiol. 13 (2015) 509–523, https://doi.org/10.1038/nrmicro3496.
[48] H.U. van der Heul, B.L. Bilyk, K.J. McDowall, R.F. Seipke, G.P. van Wezel, Regulation of antibiotic production in *Actinobacteria*: new perspectives from the postgenomic era, Nat. Prod. Rep. 35 (2018) 575–604, https://doi.org/10.1039/c8np00012c.
[49] I.M. Francis, S. Jourdan, S. Fanara, R. Loria, S. Rigali, The cellobiose sensor CebR is the gatekeeper of *Streptomyces scabies* pathogenicity, mBio 6 (2015), https://doi.org/10.1128/mBio.02018-14 e02018-14.
[50] D. Komeil, A.M. Simao-Beaunoir, C. Beaulieu, Detection of potential suberinase-encoding genes in *Streptomyces scabiei* strains and other actinobacteria, Can. J. Microbiol. 59 (2013) 294–303, https://doi.org/10.1139/cjm-2012-0741.
[51] D.R.D. Bignell, J.K. Fyans, Z. Cheng, Phytotoxins produced by plant pathogenic *Streptomyces* species, J. Appl. Microbiol. 116 (2014) 223–235, https://doi.org/10.1111/jam.12369.

[52] C.V. Vincent, D.R.D. Bignell, Regulation of virulence mechanisms in plantpathogenic *Streptomyces*, Can. J. Microbiol. 70 (2024) 199–212, https://doi.org/10.1139/cjm-2023-0171.
[53] H. Zhang, Y. Ping, X. Liu, X. He, C. Du, Pathogenic factors of plant pathogenic *Streptomyces*, Potato Res. 67 (2024) 621–646, https://doi.org/10.1007/s11540-023-09660-6.
[54] M.H. Medema, E. Takano, R. Breitling, Detecting sequence homology at the gene cluster level with MultiGeneBlast, Mol. Biol. Evol. 30 (2013) 1218–1223, https://doi.org/10.1093/molbev/mst025.
[55] J.C. NavarroMuñoz, N. SelemMojica, M.W. Mullowney, S.A. Kautsar, J.H. Tryon, E. I. Parkinson, E.L.C. De Los Santos, M. Yeong, P. CruzMorales, S. Abubucker, A. Roeters, W. Lokhorst, A. FernandezGuerra, L.T.D. Cappelini, A.W. Goering, R. J. Thomson, W.W. Metcalf, N.L. Kelleher, F. BaronaGomez, M.H. Medema, A computational framework to explore largescale biosynthetic diversity, Nat. Chem. Biol. 16 (2020) 60–68, https://doi.org/10.1038/s41589-019-0400-9.
[56] W. Kim, N. Lee, S. Hwang, Y. Lee, J. Kim, S. Cho, B. Palsson, B.K. Cho, Comparative genomics determines strain-dependent secondary metabolite production in *Streptomyces venezuelae* strains, Biomolecules 10 (2020) 864, https://doi.org/10.3390/biom10060864.
[57] A. Biessy, M. Cadieux, M. Ciotola, R. St-Onge, J. Blom, M. Filion, Virulence determinants are unevenly distributed within *Streptomyces* species and strains causing potato common scab in the province of Quebec, Canada, Plant Dis. 108 (2024) 3527–3539, https://doi.org/10.1094/PDIS-04-24-0744-RE.